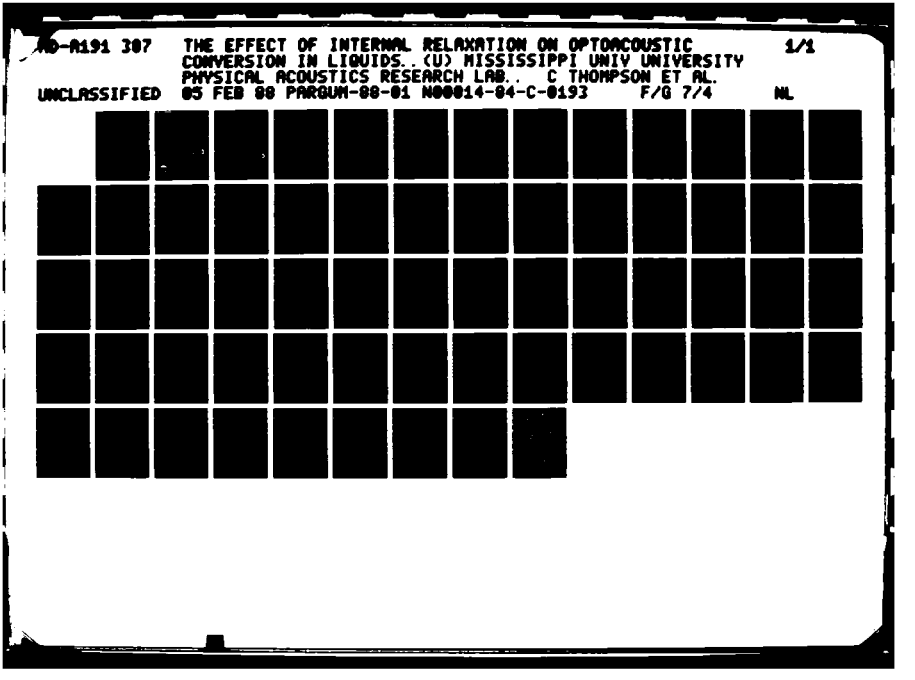
AD-A191 307 THE EFFECT OF INTERNAL RELAXATION ON OPTOACOUSTIC 1/1
CONVERSION IN LIQUIDS..(U) MISSISSIPPI UNIV UNIVERSITY
PHYSICAL ACOUSTICS RESEARCH LAB.. C THOMPSON ET AL.
UNCLASSIFIED 05 FEB 88 PARGUM-88-01 N00014-84-C-0193 F/G 7/4 NL

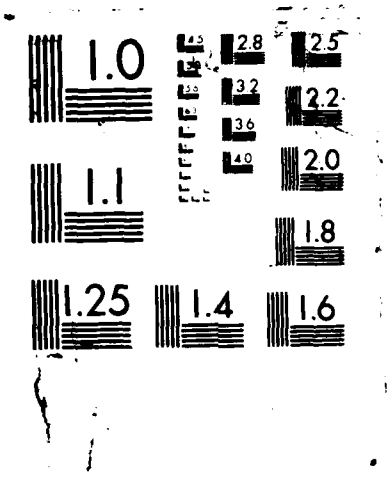
1.0
1.1
1.25
1.4
1.6
1.8
2.0
2.2
2.5
2.8
3.2
3.6
4.0

THE EFFECT OF INTERNAL RELAXATION ON OPTOACOUSTIC CONVERSION IN LIQUIDS

Charles Thompson and Henry E. Bass

Physical Acoustics Research Laboratory
University of Mississippi
University, Mississippi 38677

PARGUM 88-01

THE UNIVERSITY OF MISSISSIPPI
PHYSICAL ACOUSTICS RESEARCH GROUP
DEPARTMENT OF PHYSICS AND ASTRONOMY

(4)

THE EFFECT OF INTERNAL RELAXATION ON OPTOACOUSTIC CONVERSION IN LIQUIDS

Charles Thompson and Henry E. Bass

Physical Acoustics Research Laboratory
University of Mississippi
University, Mississippi 38677
PARGUM 88-01

5 February 1988

Technical Report
ONR Contract N00014-84-C-0193

Prepared for:

OFFICE OF NAVAL RESEARCH
DEPARTMENT OF THE NAVY
ARLINGTON, VIRGINIA 22217

UNCLASSIFIED
SECURITY CLASSIFICATION OF THIS PAGE

REPORT DOCUMENTATION PAGE

Form Approved OMB No. 0704-0188

1a. REPORT SECURITY CLASSIFICATION: UNCLASSIFIED	1b. RESTRICTIVE MARKINGS
2a. SECURITY CLASSIFICATION AUTHORITY	3. DISTRIBUTION / AVAILABILITY OF REPORT: Approved for public release; distribution unlimited
2b. DECLASSIFICATION / DOWNGRADING SCHEDULE	
4. PERFORMING ORGANIZATION REPORT NUMBER(S): PARGUM 88-01	5. MONITORING ORGANIZATION REPORT NUMBER(S)
6a. NAME OF PERFORMING ORGANIZATION: Physical Acoustics Research Laboratory; 6b. OFFICE SYMBOL (If applicable)	7a. NAME OF MONITORING ORGANIZATION: Office of Naval Research
6c. ADDRESS (City, State, and ZIP Code): Department of Physics and Astronomy University, MS. 38677	7b. ADDRESS (City, State, and ZIP Code): Physics Division, Code 1112 Arlington, VA 22217-5000
8a. NAME OF FUNDING / SPONSORING ORGANIZATION; 8b. OFFICE SYMBOL (If applicable)	9. PROCUREMENT INSTRUMENT IDENTIFICATION NUMBER: N00014-84-C-0193
8c. ADDRESS (City, State, and ZIP Code)	10. SOURCE OF FUNDING NUMBERS: PROGRAM ELEMENT NO. 61153N11; PROJECT NO.; TASK NO. 4126936; WORK UNIT ACCESSION NO.

11. TITLE (Include Security Classification): The Effect of Internal Relaxation on Optoacoustic Conversion in Liquids

12. PERSONAL AUTHOR(S): Thompson, Charles Howell and Bass, Henry E.

13a. TYPE OF REPORT	13b. TIME COVERED	14. DATE OF REPORT (Year, Month, Day)	15. PAGE COUNT
Technical	FROM N/A TO ____	5 February 1988	55

16. SUPPLEMENTARY NOTATION

17. COSATI CODES			18. SUBJECT TERMS (Continue on reverse if necessary and identify by block number)
FIELD	GROUP	SUB-GROUP	Optoacoustics, Relaxation in Fluids

19. ABSTRACT (Continue on reverse if necessary and identify by block number)

In the optoacoustic effect, optical energy is absorbed by a medium and converted to translational energy, creating an acoustic signal. In most liquids, the conversion process takes place very rapidly (ps or fs) and the nonradiative decay time is much shorter than the resulting acoustic signal. Theories have been developed, based purely on geometrical considerations, which accurately predict the optoacoustic signal in such cases. The results show that for a short pulse of optical energy the time dependance of the acoustic pressure is determined by the size and shape of the excitation zone.

This research was concerned with the actual energy transfer process and how variations in the process which exist from one liquid to another will affect the optoacoustic signal. The purpose of this study was to observe the optoacoustic signal in a situation where nonradiative decay is slow enough to compete with the geometry of the excitation zone in determining the time dependance of the acoustic pressure, and to

20. DISTRIBUTION / AVAILABILITY OF ABSTRACT: ☒ UNCLASSIFIED/UNLIMITED ☐ SAME AS RPT ☐ DTIC USERS	21. ABSTRACT SECURITY CLASSIFICATION: UNCLASSIFIED
22a. NAME OF RESPONSIBLE INDIVIDUAL: L. E. Hargrove	22b. TELEPHONE (Include Area Code): (202) 696-4221; 22c. OFFICE SYMBOL: ONR Code 1112

DD Form 1473, JUN 86 *Previous editions are obsolete.* SECURITY CLASSIFICATION OF THIS PAGE

ABSTRACT

THE EFFECT OF INTERNAL RELAXATION ON
OPTOACOUSTIC CONVERSION IN LIQUIDS

THOMPSON, CHARLES HOWELL. B.S., University of Central Arkansas, 1985. M.S., University of Mississippi, 1987. Thesis directed by Professor Henry E. Bass

In the optoacoustic effect, optical energy is absorbed by a medium and converted to translational energy, creating an acoustic signal. In most liquids, the conversion process takes place very rapidly (ps or fs) and the nonradiative decay time is much shorter than the resulting acoustic signal. Theories have been developed, based purely on geometrical considerations, which accurately predict the optoacoustic signal in such cases. The results show that for a short pulse of optical energy the time dependance of the acoustic pressure is determined by the size and shape of the excitation zone.

This research was concerned with the actual energy transfer process and how variations in the process which exist from one liquid to another will affect the optoacoustic signal. The purpose of this study was to observe the optoacoustic signal in a situation where nonradiative decay is slow enough to compete with the geometry of the excitation zone in determining the time dependance of the acoustic pressure, and to develop a model to predict the signal in such a situation.

Table of Contents

List of Tables

List of Figures

I. Introduction

The generation of acoustical energy by an optical energy source was observed by Alexander Graham Bell over one hundred years ago.[1] Since that time the optoacoustic effect has been used in investigations of optical spectroscopy[2], acoustic spectroscopy[3], and molecular energy transfer.[4] One advantage of optoacoustic generation is the lack of physical presence of a transducer in the medium. This property can be combined with optical sensing techniques such as monitoring probe beam deflection to produce a noncontact system for producing and observing acoustic signals.[5]

The explanation of the optoacoustic effect in liquids on a molecular level begins with the absorption of photons by the molecules of a fluid. Photon absorption leaves a molecule in an electronically excited state. Dissipation of this excitation energy can be accomplished by several mechanisms including nonradiative decay, radiative decay and photochemical processes. In nonradiative decay, interactions between molecules transfer the excitation energy to rotational, vibrational, or translational modes of the molecules at a finite rate. Energy in rotational or vibrational modes can in turn decay to translation. The net increase in translational energy produces a temperature rise in the fluid. If the radiation source is pulsed, the fluid

will cool following each pulse. The pressure variation which accompanies these heating and cooling cycles is observed as a series of acoustic pulses.

A finite decay time arises from relaxation effects in the energy transfer process. At equilibrium, the total energy of the fluid molecules is distributed among their external (translational) degrees of freedom and their internal degrees of freedom: electronic, vibrational and rotational modes. When optical energy is absorbed by electronic states some of the energy must flow to the other degrees of freedom in order to restore equilibrium. The structure of the molecules determines the energy levels present and how efficiently molecular interactions transfer energy. The time to reestablish equilibrium therefore varies from one substance to another.

Each energy exchange process between two molecular degrees of freedom is described by a relaxation equation of the form:

$$-\frac{dE}{dt} = \frac{1}{\tau}\left(E - E_o\right) \tag{1}$$

where E is the value of the energy in one degree of freedom, E_o is the value E would have at equilibrium, and τ is the relaxation time (defined as the time required for E to reach the value $E_o(\exp -1)$) which characterizes the process. This

equation also describes the temperature associated with each degree of freedom.

We can write the specific heat of the fluid as

$$C_p = C_{int} + C_{ext} \qquad C_{int} = \sum C_i \tag{2}$$

where C_i is the contribution to the specific heat from a particular internal degree of freedom. If we assume small temperature variation we can write

$$E - E_o = C_{ext} (T - T_o) \tag{3}$$

where T is the temperature associated with translation and T_o is the equilibrium temperature. For the external temperature, then, we have

$$- \frac{dT}{dt} = \frac{1}{\tau} (T - T_o) \, . \tag{4}$$

Depending on the time scale on which observations are made, not all of the relaxation processes will be important. For example, studies of excess ultrasonic absorption have shown that vibrational relaxation times are generally greater than rotational by a factor of about 100.[6] This means that over the period of time in which rotational relaxation occurs, little energy is exchanged by the vibrational modes and their contribution to the specific heat can be ignored. On a longer time scale, where vibrational relaxation is important, rotational modes establish equilibrium quickly

enough to be considered instantaneous so that they can be grouped with translation as an external degree of freedom.[7]

Existing treatments[8,9] of the optoacoustic effect in liquids have assumed time scales long enough that none of the relaxation processes in nonradiative decay will be observed; the transition from optical to translational energy is instantaneous. In this case the temporal profile of the observed pressure pulse is determined by factors related to the pulsed laser used as the energy source. In the theory of Lai and Young[8], the important time scales are the laser pulse length τ_p and the acoustical transit time across the beam radius $\tau_a = R/c$ where c is the acoustic velocity, and R is a measure of the laser beam radius.

The purpose of this study is to examine the optoacoustic effect on a time scale short enough to allow observation of internal relaxation effects. This requires that the relaxation effects take place over times greater than both τ_a and τ_p. The two liquids used are propanol and carbon disulfide (CS_2). They were chosen because of the large difference in vibrational relaxation times. Ultrasonic absorption measurements have shown that CS_2 has a vibrational relaxation time much longer than most liquids.[10] This makes it possible to observe both optoacoustic signals where relaxation affects the profile and those where it does not with the same experimental apparatus. Instead of changing

the time scale of the experiment, we change the time scale of the relaxation by using two liquids.

Section II describes the theory behind the experimental measurements and the development of a theoretical expression for the optoacoustic effect in CS_2.

Section III describes the experimental apparatus and the results of the measurements.

Section IV is involved with a numerical evaluation of the expression obtained in Section II.

Section V compares the results of the experiment to the numerical calculations.

II. Theory

A. Phenomenological approach

Prediction of the optoacoustic signal in CS_2 can be approached from a phenomenological point of view by comparing the energy transfer process to that of a liquid such as propanol where relaxation takes place very quickly. The observed signal in propanol is very similar to the signal predicted by Lai and Young.[8] This indicates that optical energy is converted to translational quickly, so that the pressure gradients observed are due primarily to the shape of the source. This is supported by an estimated value of the vibrational relaxation time for propanol (0.02 ps)[11] which is much shorter than τ_a or τ_p for the present experiment. For a similarly shaped source, we can expect the initial part of the signal to be the same in CS_2 because the relaxation process begins immediately upon absorption. It is during the early part of the process, when the excited states are highly populated, that the greatest amount of energy is transferred. At some point, however, the signals will begin to differ as translational energy continues to be produced in CS_2 after the populations of excited states in propanol have essentially reached equilibrium.

Consider Eq. (4) for the external temperature T. Suppose that the internal temperature T' is raised suddenly from T_o to T_1. The equilibrium value for T is also raised; therefore, energy must flow into the external degrees of

freedom to restore equilibrium. The energy can only come from the internal degrees of freedom, however, which means they do not remain at T_1. When equilibrium is restored it will be at a temperature T_2 between T_o and T_1.

Conservation of energy allows us to write[12]

$$C_{int}(T_1-T_o) = C_{int}(T'-T_o) + C_{ext}(T-T_o)$$

or

$$C_{int}(T_1-T') = C_{ext}(T-T_o) \quad . \tag{5}$$

At equilibrium,

$$C_{int}(T_1-T_2) = C_{ext}(T_2-T_o) \quad ,$$

or

$$T_2 = T_1\left(\frac{C_{int}}{C_{int} + C_{ext}}\right) + T_o\left(\frac{C_{ext}}{C_{int} + C_{ext}}\right)$$

which gives

$$T_2 = T_1 \frac{C_{int}}{C_p} + T_o \frac{C_{ext}}{C_p} \quad . \tag{6}$$

The differential equation for T is

$$-\frac{dT}{dt} = \frac{1}{\tau}(T-T') \quad . \tag{7}$$

Adding $C_{int}T$ to both sides of Eq. (5) we have

$$C_{int}T + C_{int}T_1 - C_{int}T' = C_pT - C_{ext}T_o$$

or

$$T-T' = \frac{C_p}{C_{int}} \left(T - \frac{C_{ext}}{C_p} T_o - \frac{C_{int}}{C_p} T_1 \right)$$

so

$$T-T' = \frac{C_p}{C_{int}} (T-T_2) \quad . \tag{8}$$

Substituting this in Eq. (7) we have

$$-\frac{dT}{dt} = \frac{1}{\tau} \frac{C_p}{C_{int}} (T-T_2) \quad . \tag{9}$$

The observed relaxation time, thus, is not τ but

$$\tau' = \frac{C_{int}}{C_p} \tau \quad .$$

With the use of Eq. (3) we have

$$-\frac{dE}{dt} = \frac{1}{\tau'} (E-E_2)$$

which has the solution

$$E = E_2 \left(1-e^{-t/\tau'}\right) \tag{10}$$

or

$$\frac{dE}{dt} = \frac{E_2 e^{-t/\tau'}}{\tau'} \quad . \tag{11}$$

This means that the translational energy which appears per

unit time decays exponentially with relaxation time τ'. Experimentally then, we should expect to see an exponential decay superimposed on a signal due to the shape of the source.

The above assumes that all of the internal degrees of freedom have the same relaxation time. In real systems, there are multiple processes taking place simultaneously. The next section discusses a method to treat multilevel systems.

B. Relaxation Equation

In 1972 Bauer[13] introduced a theory accounting for energy transfer processes which affect the optoacoustic signal in multilevel systems. The matrix notation involved is well suited to numerical calculations and can be used to describe the effect of an arbitrary number of optical and collisional transitions. His formulation assumes gas phase interactions but is applicable to liquid with minor changes. The collisional transitions which result in energy transfer are of the form

$$M_i + M_j \underset{k_\alpha'}{\overset{k_\alpha}{\leftrightarrow}} M_k\ M_l \tag{12}$$

where i...l include any energy level of the fluid, and k_α and k_α' are the forward and backward rates of reaction α. Bauer introduces a set of progress variables ξ_α so that

$$\dot{\xi}_\alpha = n\left(k_\alpha x_i x_j - k_\alpha' x_k x_l\right) \tag{13}$$

where n is the total number of molecules and $x_i...x_1$ are the mole fractions. This equation has been modified to eliminate the pressure p which is applicable only for gases.

Assuming small perturbations, $\dot{\xi}_\alpha$ is expanded about equilibrium. A matrix notation is then introduced which allows summation of all the coupled reaction equations into a single equation for the collisional change in population number, $\dot{n}_{coll}$. Since the change in population is a measure of how much energy is exchanged between the internal and external degrees of freedom, $\dot{n}_{coll}$ can be related to the temperature variation. The matrix equation is then solved for the temperature variation as a sum of terms, each with a particular relaxation time, τ, and amplitude, A.

CS_2 has been modeled as a three level system, as shown in Figure 1. The highest level is the electronic state which is excited optically. It is given an energy of 2.96 X 10^4 cm^{-1} above the ground state to correspond to the frequency of the nitrogen laser radiation. Between this level and the ground state is included a vibrational mode which is doubly degenerate. Its energy is 397 cm^{-1}.[14] Although there are other vibrational modes present in CS_2, Andreae et. al.[10] have shown that relaxation of the vibrational specific heat of CS_2 can be adequately described by a single relaxation time which they measured to be 2.04 ns. The rate k_{10} has therefore been given the value that they measured and the other modes have been neglected. The other two rates, k_{20} and

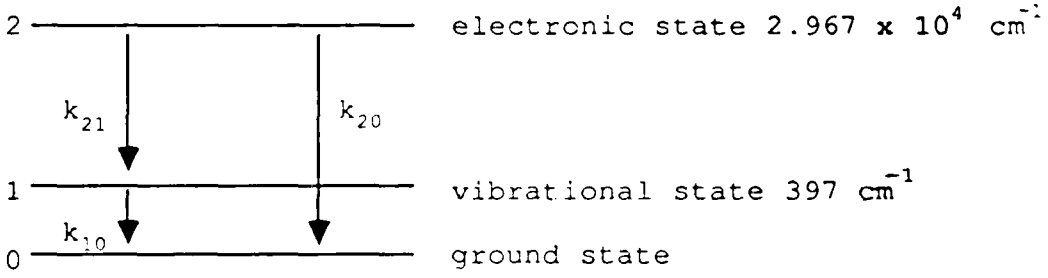
2
electronic state 2.967 x 10^4 cm^-1
k21
k20
1
vibrational state 397 cm^-1
k10
0
ground state

Figure 1

k_{21}, will be varied later to give the best fit to experimental data.

With a three level system and one conservation law (conservation of total number of molecules) a double relaxation process is expected. Solution of the coupled reaction equations results in two relaxation times, τ_1 and τ_2, and two relaxation strengths, A_1 and A_2. Calculation of these values was accomplished with the use of a program written by Manaf Ali in 1985 for his dissertation.[15] The program was originally compiled to calculate pulsed spectrophone response in sulfur hexafluoride using the Bauer matrix notation. It was therefore easily modified to the present application.

C. Wave Equation

According to Hutchins and Tam[5], we can write the inhomogeneous wave equation for the optoacoustic pressure as

$$\left(\frac{1}{c^2}\frac{\partial^2}{\partial t^2} - \nabla^2\right) p = \left(K_A \frac{\partial}{\partial t} + K_E \frac{\partial^2}{\partial t^2}\right) I \tag{14}$$

where p is the acoustic pressure, I the laser intensity, and c the acoustic velocity. The first term on the right hand side of Eq. (14) is due to thermal expansion where

$$K_A = \frac{\alpha\beta}{C_p} \tag{15}$$

α is the optical absorption coefficient, β is the volume

expansivity and C_p is the specific heat at constant pressure. The second term is due to electrostriction where

$$K_E = \frac{-\gamma}{2nc_L c^2} , \tag{16}$$

γ is the electrostrictive coefficient, n is the index of refraction, and c is the speed of light in a vacuum.

If we introduce a potential function, $\phi(\mathbf{r},t)$, that satisfies

$$\left(\frac{1}{c^2}\frac{\partial^2}{\partial t^2} - \nabla^2\right)\phi(\mathbf{r},t) = I(\mathbf{r},t) \tag{17}$$

then we can write the acoustic pressure as a sum of thermal expansion and electrostrictive terms given by

$$p_A = K_A \frac{\partial \phi}{\partial t} \tag{18}$$

and

$$p_E = K_E \frac{\partial^2 \phi}{\partial t^2} = \frac{K_E}{K_A}\frac{\partial p_A}{\partial t} . \tag{19}$$

In the present case the ratio of K_E to K_A is small so that we will ignore the electrostrictive pressure component.

Using the laser intensity as the source function in the wave equation ignores the effects of internal relaxation in

optoacoustic conversion. It is instructional, however, to note results obtained with this procedure. Lai and Young[8] have investigated cases of weak absorption where the spatial length of the source is much longer than the perpendicular distance to the observation point so that the problem is essentially two dimensional. The laser pulse intensity can be considered as a product of radial and spatial profiles characterized by τ_a and τ_p respectively as defined in the introduction. If both profiles are given Gaussian forms and $\tau_p << \tau_a$, as in the present case, then the resulting pressure profile is relatively insensitive to τ_p. The rise and decay of the potential function and therefore the peaks in pressure ($\partial\phi/\partial t$) are governed primarily by the spatial profile of the absorbing region.

We have modeled the source term for the present experiment by replacing the time dependence of the laser pulse with the term

$$\frac{A_1}{\tau_1} e^{-t/\tau_1} + \frac{A_2}{\tau_2} e^{-t/\tau_2} \tag{20}$$

where A_1, A_2 are the relaxation strengths and τ_1, τ_2 are the relaxation times discussed in the previous section. With a Gaussian radial profile of radius a, and the pulse propagating along the z-axis, we now write the source term as

$$I(r,t) = \left(\frac{A_1}{\tau_1} e^{-t/\tau_1} + \frac{A_2}{\tau_2} e^{-t/\tau_2}\right) e^{-r^2/a^2 - \alpha z} \tag{21}$$

which accounts for internal relaxation as well as a finite absorption coefficient. In effect, this gives the laser pulse a flat temporal profile (an instantaneous rise time at t=0). The rise in the potential will be governed by the spatial profile as it would in the absence of relaxation, since $\tau_p << \tau_a$. The decay, however, will depend on the relationship of τ_a to τ_1 and τ_2. With the Gaussian radial distribution defined this way, the R defined by Lai and Young[8] is equal to $a/\sqrt{2}$. τ_a is therefore equal to $a/\sqrt{2}c$. In this form αI is the translational energy per unit time per unit volume which appears in the liquid. Combining Eq. (17) and (21) we have

$$\left(\frac{1}{c^2}\frac{\partial^2}{\partial t^2} - \nabla^2\right)\phi = \left(\frac{A_1}{\tau_1}e^{-t/\tau_1} + \frac{A_2}{\tau_2}e^{-t/\tau_2}\right)e^{-r^2/a^2}e^{-\alpha z} \tag{22}$$

The general form of this equation is

$$\left(\frac{1}{c^2}\frac{\partial^2}{\partial t^2} - \nabla^2\right)\psi = 4\pi q(\mathbf{r},t) \tag{23}$$

where $q(\mathbf{r},t)$ is the source strength.

The solution, using Green's function, is[16]

$$\psi(\mathbf{r},t) = \frac{1}{4\pi}\int dV_o \frac{q(\mathbf{r}_o, t - R/C)}{R} \tag{24}$$

where $|\mathbf{r}_o| = (r_o^2+z_o^2)^{1/2}$ is the position of the source point, $R = |\mathbf{r}-\mathbf{r}_o|$, and the integrated volume includes the spatial extent of the source as well as any image sources necessary

to meet boundary conditions.

In this experiment, the test cell containing the liquid is large enough that no reflections from the walls are observed until well after the original signal. We therefore ignore boundary effects except for the surface through which the laser pulse enters the fluid. Boundary conditions at this surface are met by including a mirror image of the real source at negative values of z_o.

Comparing Eq. (17) and (23)

$$q(\mathbf{r},t) = \frac{1}{4\pi} I(\mathbf{r},t) . \tag{25}$$

Inserting this and Eq. (21) into Eq. (24), we have

$$\phi(\mathbf{r},t) = \frac{1}{(4\pi)^2} \int dV_o \frac{e^{-r_o^2/a^2 - \alpha z_o}}{R} \left(\frac{A_1}{\tau_1} e^{-(t - R/C)/\tau_1} + \frac{A_2}{\tau_2} e^{-(t - R/C)/\tau_2} \right) \tag{26}$$

or

$$\phi(\mathbf{r},t) = \frac{1}{(4\pi)^2} \int \frac{dV_o}{R} g(\mathbf{r}_o) f(t - R/C) \tag{27}$$

where

$$g(\mathbf{r}_o) = \exp\left(-r_o^2/a^2 - \alpha z_o\right) \tag{28}$$

is the spatial profile function, and

$$f(t) = \frac{A_1}{\tau_1} e^{-t/\tau_1} + \frac{A_2}{\tau_2} e^{-t/\tau_2} \tag{29}$$

is the temporal profile function.

III. Experiment

The experimental apparatus used in this study consists basically of a pulsed nitrogen (N_2) laser used as the energy source to create optoacoustic pulses, a continuous wave Helium-Neon laser which probes the refractive index gradient produced by the acoustic pulse, and a photodetector to monitor the probe beam. These optical components are mounted on a Newport Research Corporation table top and vibration isolation system as shown in Figure 2. The N_2 laser is a model LN1000 atmospheric pressure laser manufactured by PRA, Inc. It produces pulses of 1 mJ energy and 800 ps duration for a peak power of 1.25 MW at 337 nm wavelength. The pulse is collimated and then focused into a quartz fluorimeter cell, which contains the liquid sample, mounted on a translation stage. The lenses used in the laser path are fused silica, and the mirror is a silver coated front surface reflector. The laser pulse's original cross section is rectangular, 3 mm X 6 mm. Its size as it enters the test cell is controlled by the focal length of the focusing lens. The maximum energy entering the test cell per pulse is about 0.36 mJ. The pulse energy can be varied by placing glass microslides in the laser path. Each glass slide absorbs a small percentage of the energy in the pulse. Most of the data taken in CS_2 is at a pulse energy of about 26.3 μJ.

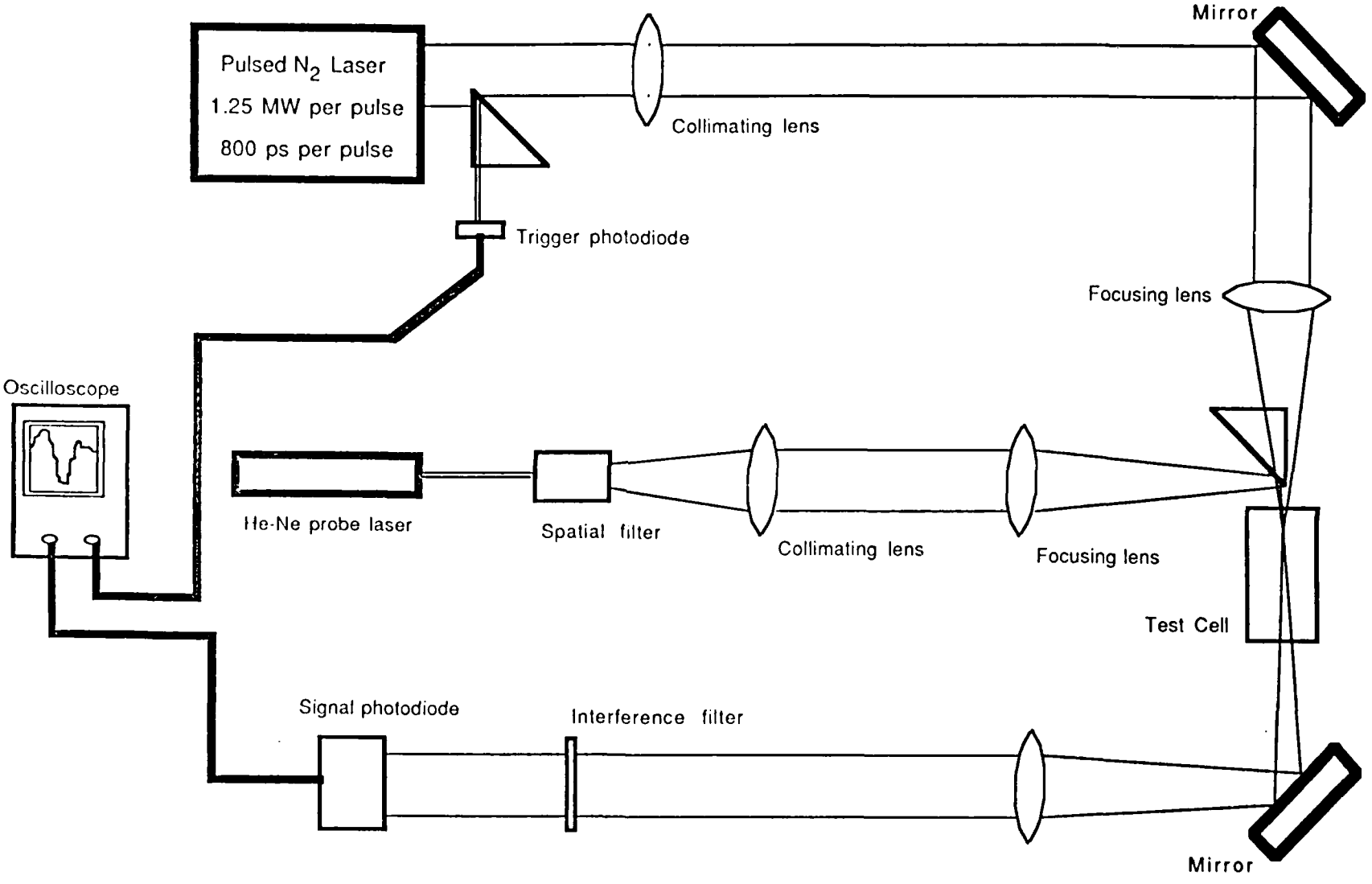
Pulsed N_2 Laser
1.25 MW per pulse
800 ps per pulse
Collimating lens
Mirror
Trigger photodiode
Focusing lens
Oscilloscope
He-Ne probe laser
Spatial filter
Collimating lens
Focusing lens
Test Cell
Signal photodiode
Interference filter
Mirror

Figure 2

These values were measured with a Molectron J3-09 Joule meter and JD1000 Joule meter display.

The laser pulse is absorbed by the liquid in accordance with Beer's law and produces an outgoing acoustic pulse. The acoustic signal is observed with a probe beam deflection technique as described by Sullivan and Tam.[17] The probe laser is a Spectra Physics model 106-1 He-Ne laser of 10.0 mW output power at 632.8 nm. The beam is spatially filtered and then collimated at a diameter of approximately 15 mm. It is then focused into the test cell by a lens of 350 mm focal length producing a beam waist of about 18 μm. A silver coated prism reflects the converging beam into the test cell so that it propagates above and parallel to the ultraviolet pulse as they enter the cell.

The pressure gradient in the acoustic pulse is accompanied by a gradient in the index of refraction. As the acoustic pulse crosses the probe beam, the changing index of refraction causes a deflection of the beam which is proportional to the gradient of the acoustic pressure

$$\Gamma(\mathbf{r},t) = \frac{1}{n_o}\frac{\partial n(\mathbf{r},t)}{\partial r} \alpha \frac{\partial P(\mathbf{r},t)}{\partial r} , \tag{30}$$

where $\Gamma(\mathbf{r},t)$ is the angular deflection, n_o is the normal index of refraction, $n(\mathbf{r},t)$ is the changing index of refraction which is proportional to $P(\mathbf{r},t)$, the acoustic

pressure. Over a length of the probe beam d, the cumulative angular deflection is

$$\Gamma_{cum}(r,t) \alpha \int_0^d \frac{\partial}{\partial r} P(\mathbf{r},t)\, dz$$

$$\alpha \frac{\partial}{\partial r} \int_0^d P(\mathbf{r},t)\, dz \quad . \tag{31}$$

The probe beam continues through the test cell and through a lens which is used to control the diameter of the beam at the position of the photodiode. An interference filter is used to block any scattered light from the pulsed laser. The photodiode is placed so that any beam deflection changes its position in the beam's radial intensity distribution, which is assumed to be Gaussian. Positioning the photodiode on the steepest part of the Gaussian distribution assures that the intensity change is approximately linear with beam deflection and produces a maximum change in intensity for a given angular deflection.

The output from the photodiode, S(t), can be related to the angular deflection of the probe beam by

$$S(r,t) = GI_p'(r_d)\ L\ \Gamma_{cum} \tag{32}$$

where G is a constant which depends on the sensitivity of the photodiode, $I_p'(r_d)$ is the lateral spatial derivative of the intensity at r_d, the photodiode position, and L is the

distance from the test cell to the photodiode. From equations (31) and (32) we have

$$S(r,t) \alpha \frac{\partial}{\partial r} \int_0^a P(\mathbf{r},t)\, dz. \tag{33}$$

Therefore, when the signal is displayed on an oscilloscope, we observe the gradient of the acoustic pressure. In terms of the potential function defined in section II

$$S(r,t) \alpha \frac{\partial}{\partial r} \frac{\partial}{\partial t} \int_0^a \phi(\mathbf{r},t)\, dz. \tag{34}$$

The signal is digitized with a Tektronix 7854 storage oscilloscope which is triggered by a signal from a second photodiode upon which a small portion of the laser pulse is directed. The oscilloscope is interfaced with a Digital Equipment Corporation Minc-23 mini computer where the data is stored and analyzed.

To observe internal relaxation effects it is important that the pulse cross-section be as small as possible as it enters the test cell so that τ_a is smaller than τ_1 and τ_2. A short focal length lens is therefore desirable to focus the laser pulse into the cell. The shortest that could be used with this arrangement was 15 mm because of the prism necessary to reflect the probe beam into the cell.

Since propanol is transparent to the nitrogen laser pulse, it was necessary to add a dye which would absorb the ultraviolet and still permit passage of the Helium-Neon probe beam. Enough dye was added to make the penetration depth similar to that of CS_2 which absorbs strongly at 337 nm. With similar penetration depths the only difference between the signals observed in the two liquids should be due to the difference in sound speed and internal relaxations.

Typical waveforms in both liquids are shown in Fig. 3. To account for the differences in sound speed we compare the two signals on a scale of ct. In Fig. 3 ct = 0.0 is the time at which the oscilloscope was triggered. As expected, the early portion of the signals are similar. Following this initial rise, however, the CS_2 signal decays more slowly and reaches its minimum at a slightly later time. The pressure gradient in CS_2 is smaller in magnitude than in propanol, most of the time.

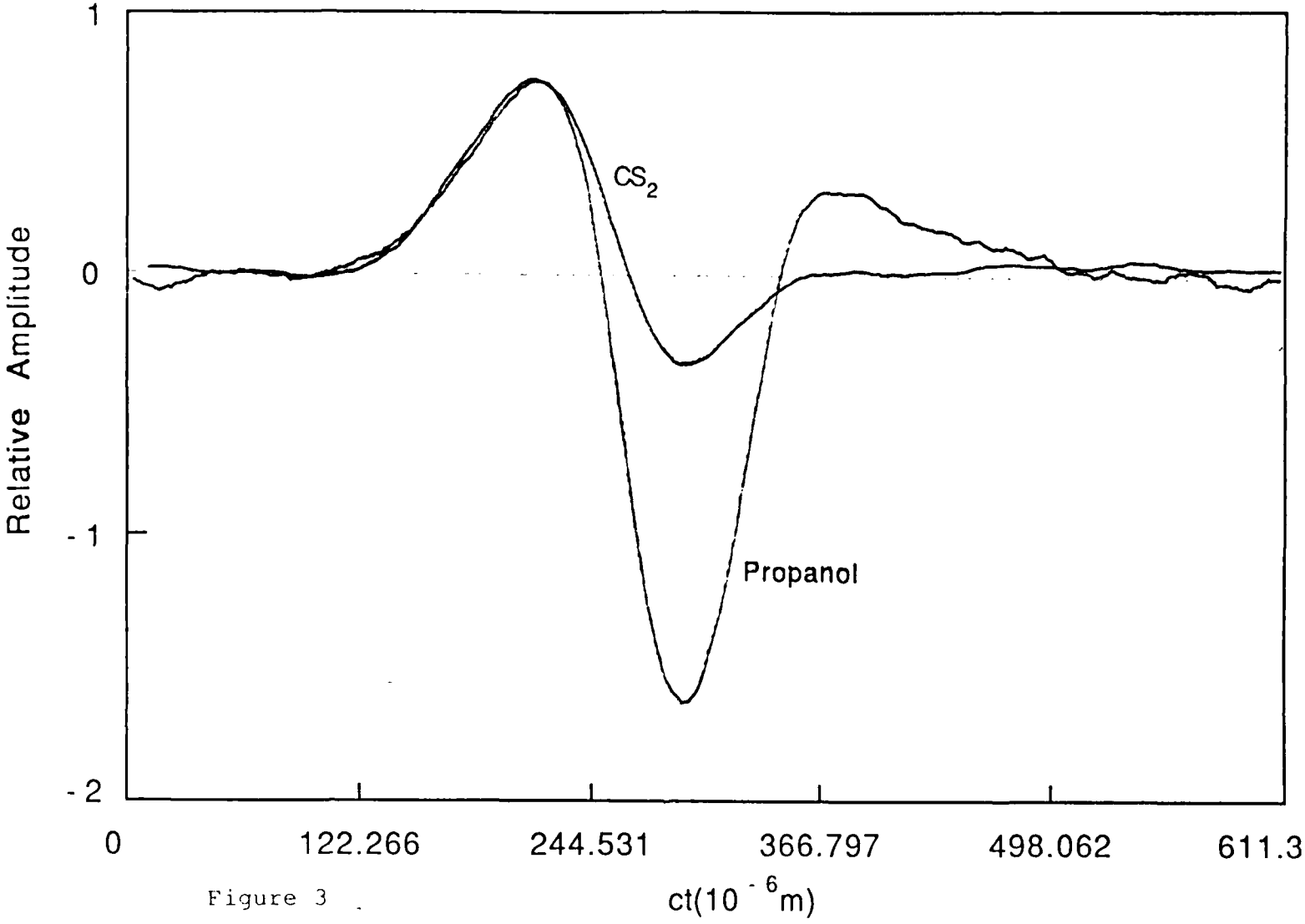
1
0
-1
-2
Relative Amplitude
CS_2
Propanol
0
122.266
244.531
366.797
498.062
611.328
ct(10^{-6}m)

Figure 3

IV. Numerical Calculations

A. Optoacoustic Signal

From equation (34) the expression we compare to the experimental signal is

$$\frac{\partial}{\partial r}\frac{\partial}{\partial t}\int_0^d \phi\ (\mathbf{r},t)\ dz\ . \tag{35}$$

If we define

$$\Phi\ (r,t) = \int_0^d \phi(\mathbf{r},t)\ dz \tag{36}$$

and use equation (27), then

$$\Phi(r,t) = \int_0^d dz\ \frac{1}{(4\pi)^2}\int dV_o\ \frac{q\ (\mathbf{r}_o)\ f\ (t - R/c)}{R}\ . \tag{37}$$

If we define a function $u(\mathbf{r},t)$ by

$$u(\mathbf{r},t) = \frac{1}{(4\pi)^2}\int dV_o\ \frac{g(\mathbf{r}_o)}{R}\ \delta(t - R/c) \tag{38}$$

and define the Dirac response of the probe beam by

$$U\ (r,t) = \int_0^d u(\mathbf{r},t)\ dz \tag{39}$$

then

$$\Phi(r,t) = \int_0^t U(r,t-t')\ f(t')\ dt'. \tag{40}$$

Writing Φ in terms of U saves time in the numerical evaluation of Φ because the spatial integration need only be done once rather than at each point in time. $\mathbf{u}(\mathbf{r},t)$ represents the potential due to a source with spatial dependance $g(\mathbf{r}_o)$, which exists only at t=0. The integral of $\mathbf{u}(\mathbf{r},t)$ over z represents the effect upon a length d of the probe beam. The convolution of the resulting function with the actual time dependence of the source produces the potential at any later point in time.

Evaluation of $\mathbf{u}(\mathbf{r},t)$ is accomplished by integrating over all space in a spherical coordinate system with its origin at the observation point. Defining dV_o by

$$dV_o = R^2 \sin\theta \; dR \; d\theta \, d\phi = R^2 dR \; d\Omega \tag{41}$$

we have

$$u(\mathbf{r},t) = \frac{1}{(4\pi)^2} \int_0^{\infty}\int_{\Omega} R \; dR \; d\Omega \, g(\mathbf{r}_o) \; \delta(t - R/c) \; . \tag{42}$$

It is possible to show that

$$\delta(t - R/c) = c\delta(ct - R) \tag{43}$$

therefore,

$$u(\mathbf{r},t) = \frac{c^2 t}{(4\pi)^2} \int_0^{\infty}\int_{\Omega} R \; dR \; d\Omega \, g(\mathbf{r}_o) \; \delta(ct - R) \; . \tag{44}$$

The integrand is zero except when R = ct, therefore

$$u(\mathbf{r},t) = \frac{c^2 t}{(4\pi)^2} \int_{\Omega} g(\mathbf{r}_o)\, d\Omega, \tag{45}$$

or

$$u(\mathbf{r},t) = \frac{c^2 t}{(4\pi)^2} \int_0^{2\pi}\int_0^{\pi} g(\mathbf{r}_o)\, \sin\theta\, d\theta\, d\phi \tag{46}$$

Defining $\chi = \cos\theta$, $d\chi = -\sin\theta\, d\theta$,

$$u(\mathbf{r},t) = \frac{c^2 t}{(4\pi)^2} \int_0^{2\pi}\int_{-1}^{1} g(\mathbf{r}_o)\, d\chi\, d\phi. \tag{47}$$

A point in time t defines a sphere of radius R=ct about the observation point $|\mathbf{r}| = (r^2+z^2)^{1/2}$. $u(\mathbf{r},t)$ is the sum of the contributions from all source points which lie on the surface of this sphere. In the numerical calculations, knowledge of the source has been used to modify the limits of integration. By defining $g(\mathbf{r}_o)$ to be zero for $r_o > 4a$ and $z_o > 20/\alpha$, definite limits for χ and ϕ are calculated for each value of $\mathbf{r}$ and t. The length of the probe beam considered was determined by calculating the farthest point along its length that would be affected by the source at the final time of interest. The programs which calculate U(r,t) and Φ(r,t) are located in the appendices. The pressure $\left(\frac{\partial}{\partial t}\,\Phi(r,t)\right)$ and its gradient $\left(\frac{\partial}{\partial r}\,\frac{\partial}{\partial t}\,\Phi(r,t)\right)$ are also calculated numerically by programs in the appendices.

B. Curve Fitting Procedure

The procedure for producing the theoretical curves was to begin with very short relaxation times so that the signal is dominated by the spatial characteristics of the excitation beam. These characteristics were varied until the result matched the observed signal in propanol which is known to have a very short relaxation time. Relaxation times and strengths were then calculated using the known rate for the vibration to translation transition, k_{10}, and assumed rates of transition from the electronic state. Varying the values of k_{20} and k_{21} changed the relaxation times and strengths. These two rates were varied until the resulting relaxation strengths and times gave an optoacoustic signal which most closely resembled the observed signal in CS_2.

V. Discussion and Conclusion

The results of this study show that internal relaxation can indeed be important in determining the time dependence of the optoacoustic signal in liquids.

A good representation of the signal observed in propanol was obtained by assigning a rate of 490.2 X 10^6 s^{-1} to each of the three transitions. The resulting relaxation times were 1.02 ns and 1.47 ns. The pressure gradient obtained with these relaxation times is shown in Fig. 4 along with the experimental curve. Here the time scale is for the theoretical curve. The experiemntal curve is overlaid so that the peaks occur at the same point in time. Performing the calculation with even shorter relaxation times results in the same theoretical curve, indicating that with these relaxation times the signal is determined entirely by the spatial characteristics of the excitation pulse. The value of "a" in this calculation was 50 μm giving the radius a value of approximately 71 μm at the exp(-2) value of the intensity. The tbeory of Heritier[9] predicts that the time separation of the positive and negative pressure peaks, which is approximately the time separation of the points where the gradient goes through zero, will be[17]

$$\Delta t = 1.66 \left(\tau_p^2 + \frac{\omega_s^2}{2c^2} \right)^{1/2} ,$$

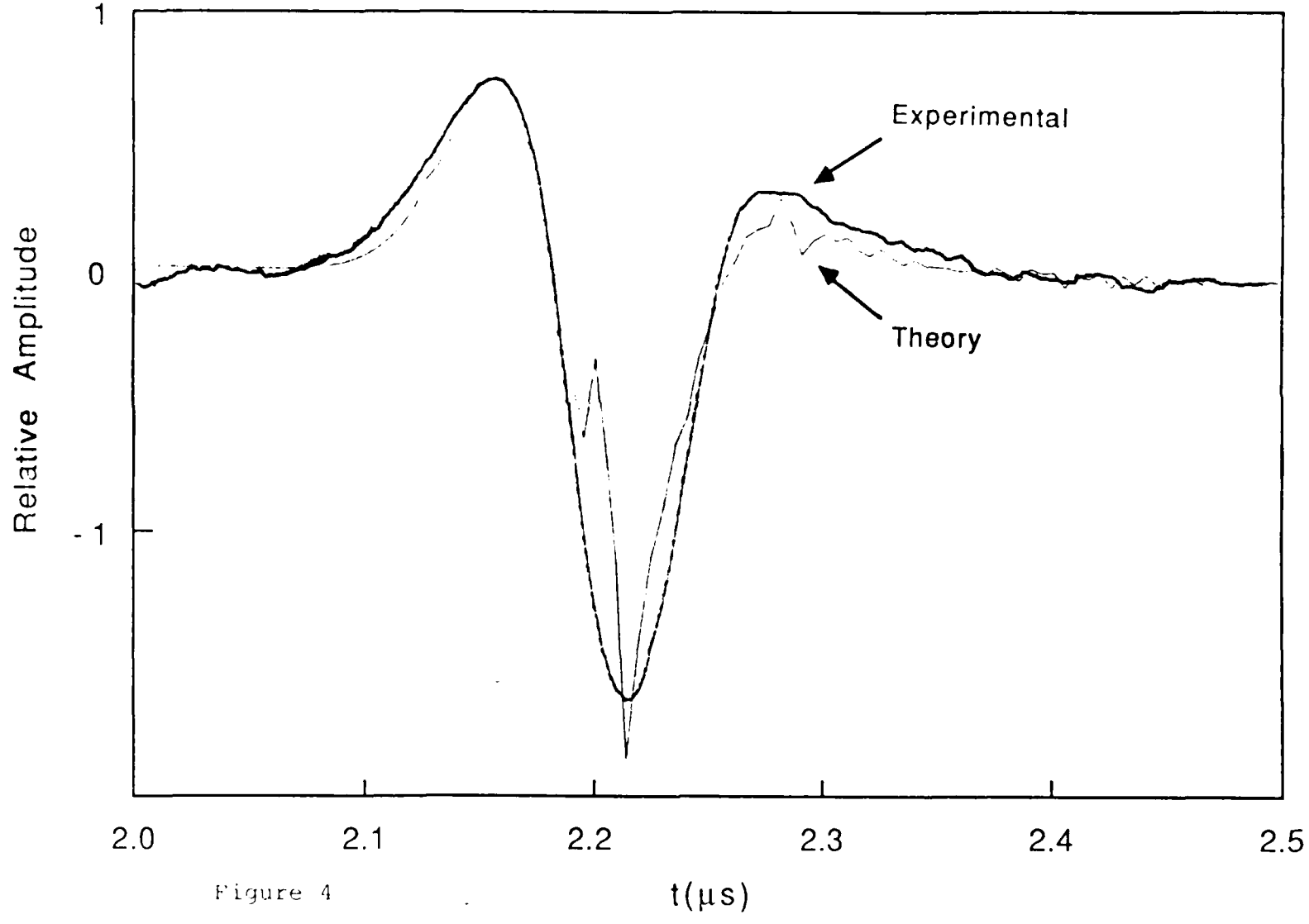
1
0
-1
Relative Amplitude
Experimental
Theory
2.0
2.1
2.2
2.3
2.4
2.5
t(μs)

Figure 4

where ω_o is the radius at which the intensity is down by exp(-2). For the present case with τ_p = 0.8 ns, ω_o = 71μm and c = 1223 m/s for propanol, Δt should be 68.3 ns. The actual time separation in the experimental waveform is 72.3 ns. The discrepancy in the initial rise of the curves in Fig. 4, which begins earlier in the experimental curve and shows a more gradual change, is probably due to the fact that the laser pulse is not Gaussian as modeled. The roughness of the computed waveform can be traced to edge effects in the source function caused by truncating the Gaussian distribution at $r_o = 4a$ and $z_o = 20/\alpha$. These effects are magnified in the process of taking two numerical derivatives of the calculated function, Φ. Both of these problems can probably be corrected by modifying the spatial profile function, Eq. (28). However, the overall time dependence of the pulse is well represented by the theory. It should be noted that to avoid noise during the experimental signal digitization, the band width of the oscilloscope was reduced to 20 MHz. Had a similar filter been used in the numerical calculations, the agreement might be different.

Table 1 shows combinations of values assigned to the rates k_{21}, k_{10}, and k_{20} and the resulting amplitudes and relaxation times. Theoretical wave forms calculated using these parameters are shown in Figs. 5 through 8.

Table 1

Figure	Rates in 10^6 s^{-1}			A_1	A_2	τ_1 ns	τ_2 ns
	k_{21}	k_{10}	k_{20}				
5	490.2	490.2	490.2	-1.26×10^{-5}	2.03×10^{-4}	1.47	1.02
6	26.86	490.2	16.86	-1.26×10^{-5}	2.03×10^{-4}	1.47	22.8
7	26.86	490.2	.5686	-1.26×10^{-5}	2.03×10^{-4}	1.47	36.5
8	.2686	490.2	10.67	-1.26×10^{-5}	2.03×10^{-4}	1.47	91.4

With the value of k_{10} held constant to correspond to the accepted value of the vibrational relaxation time of CS_2, the amplitudes and τ_1 also remain constant. Table 1 is arranged to show rate combinations which give increasing values of τ_2. These results are not unique, however. For instance, the last value of τ_2, 91.4 ns, also results from setting k_{21} = 10.37 X 10^6 s^{-1} and k_{20} = .5686 X 10^6 s^{-1}.

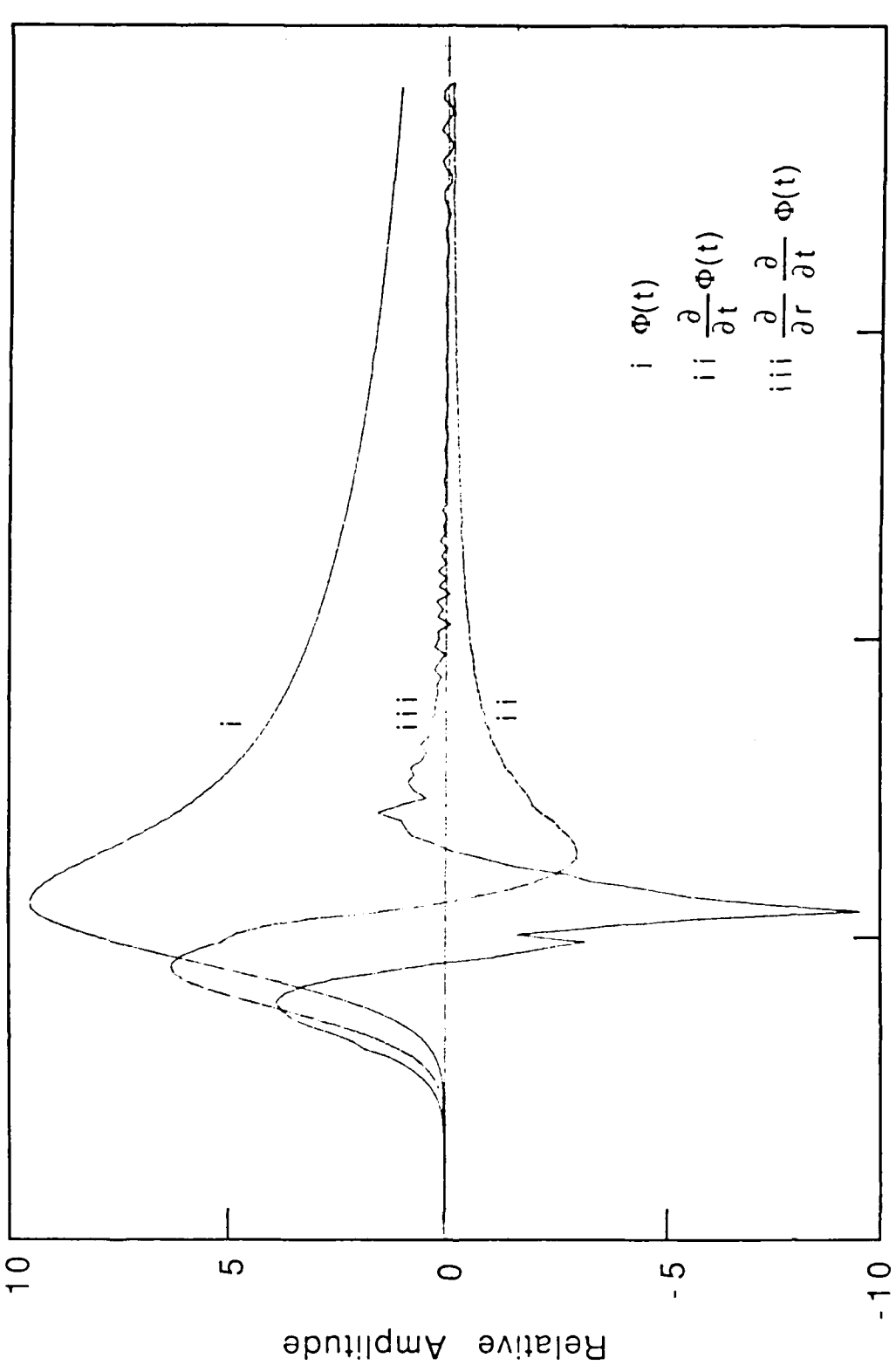
Relative Amplitude
10
5
0
-5
-10
2
2.2
2.4
2.6
2.8
t(μs)
i
iii
ii
i Φ(t)
ii ∂/∂t Φ(t)
iii ∂/∂r ∂/∂t Φ(t)

Figure 5

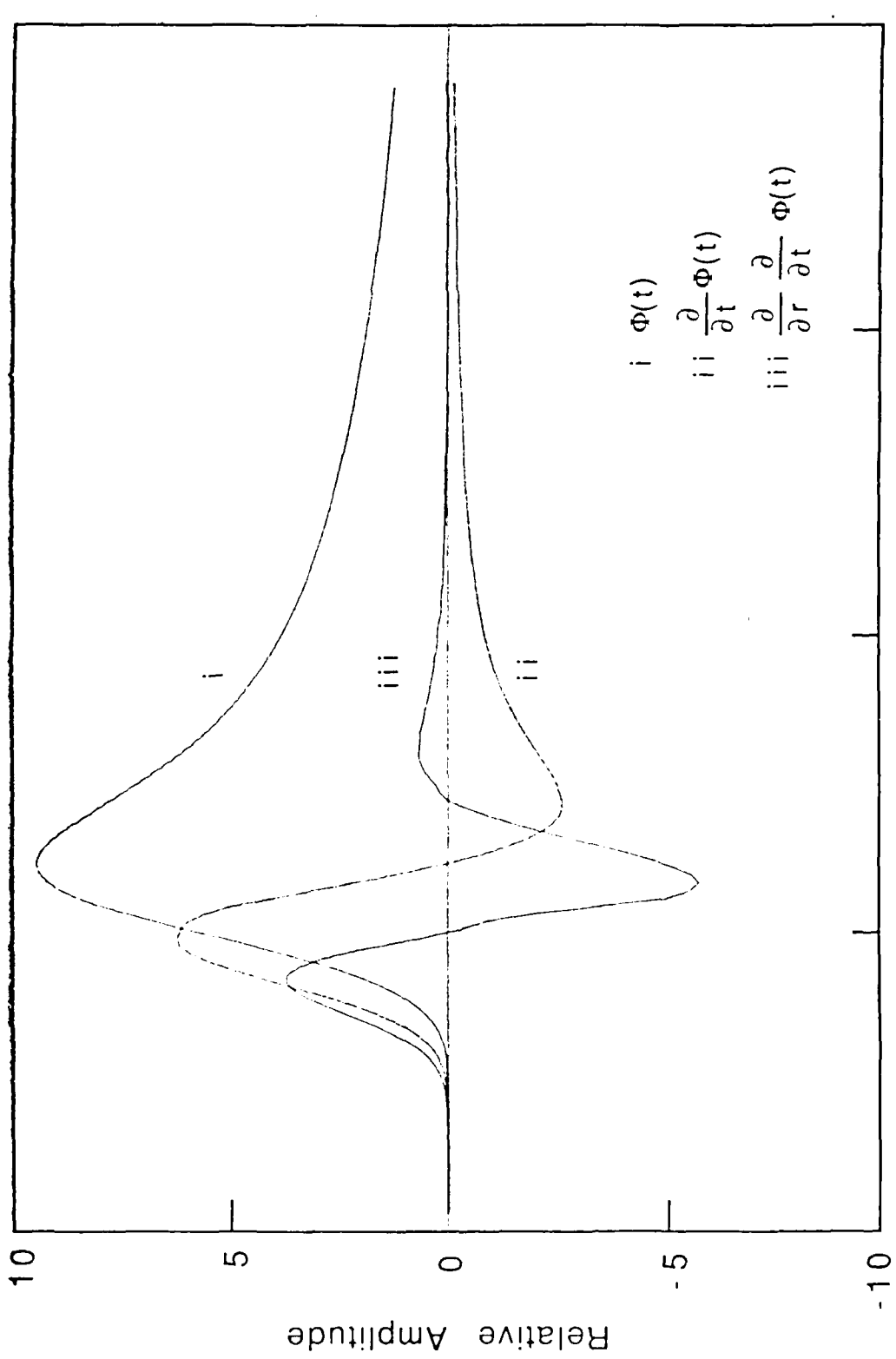
Relative Amplitude
10
5
0
-5
-10
2
2.2
2.4
2.6
2.8
t(μs)
i
iii
ii
i Φ(t)
ii ∂/∂t Φ(t)
iii ∂/∂r ∂/∂t Φ(t)

Figure 6

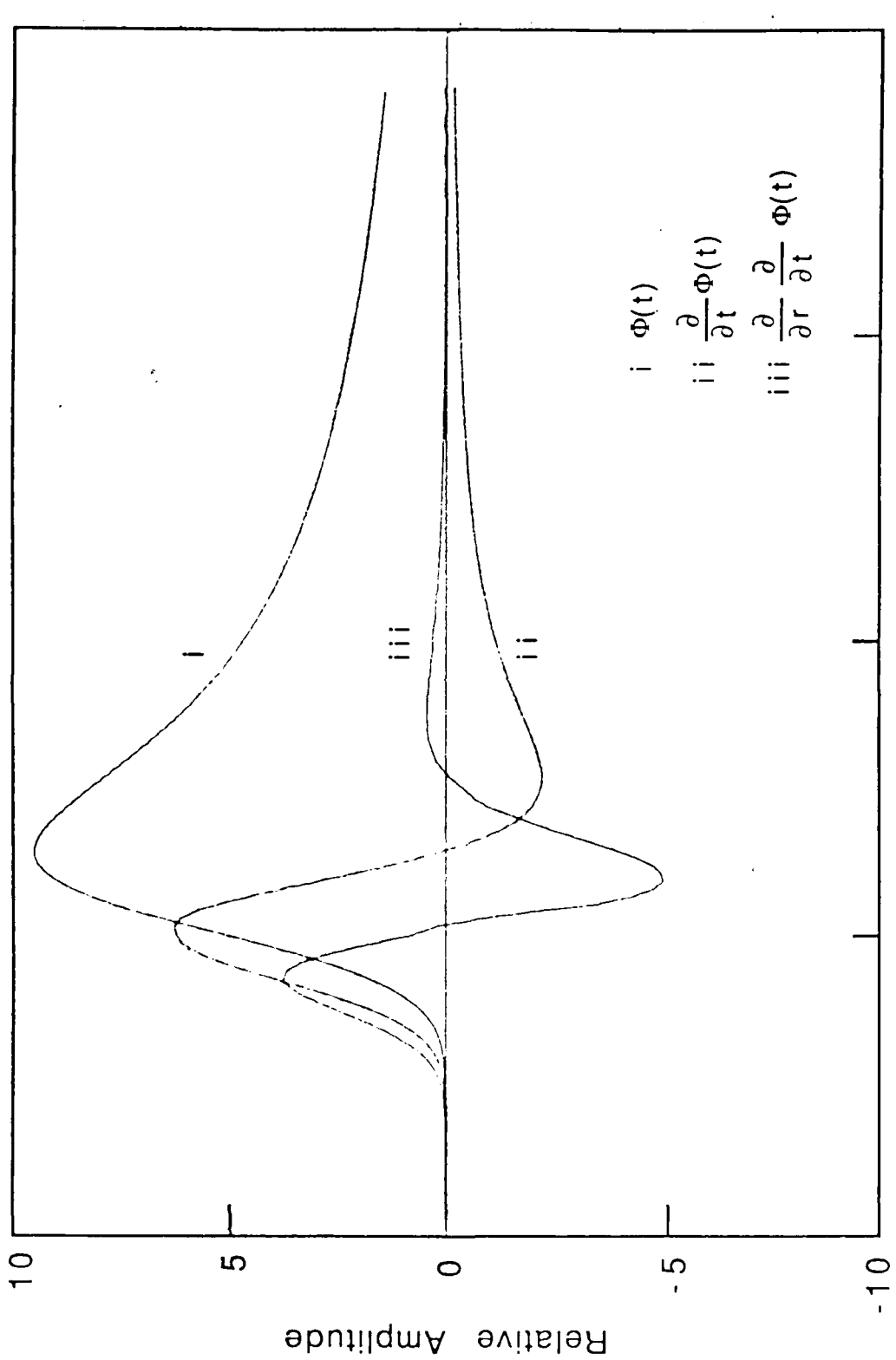
Relative Amplitude
10
5
0
-5
-10
2
2.2
2.4
2.6
2.8
t(μs)
i
ii
iii
i Φ(t)
ii ∂/∂t Φ(t)
iii ∂/∂r ∂/∂t Φ(t)

Figure 7

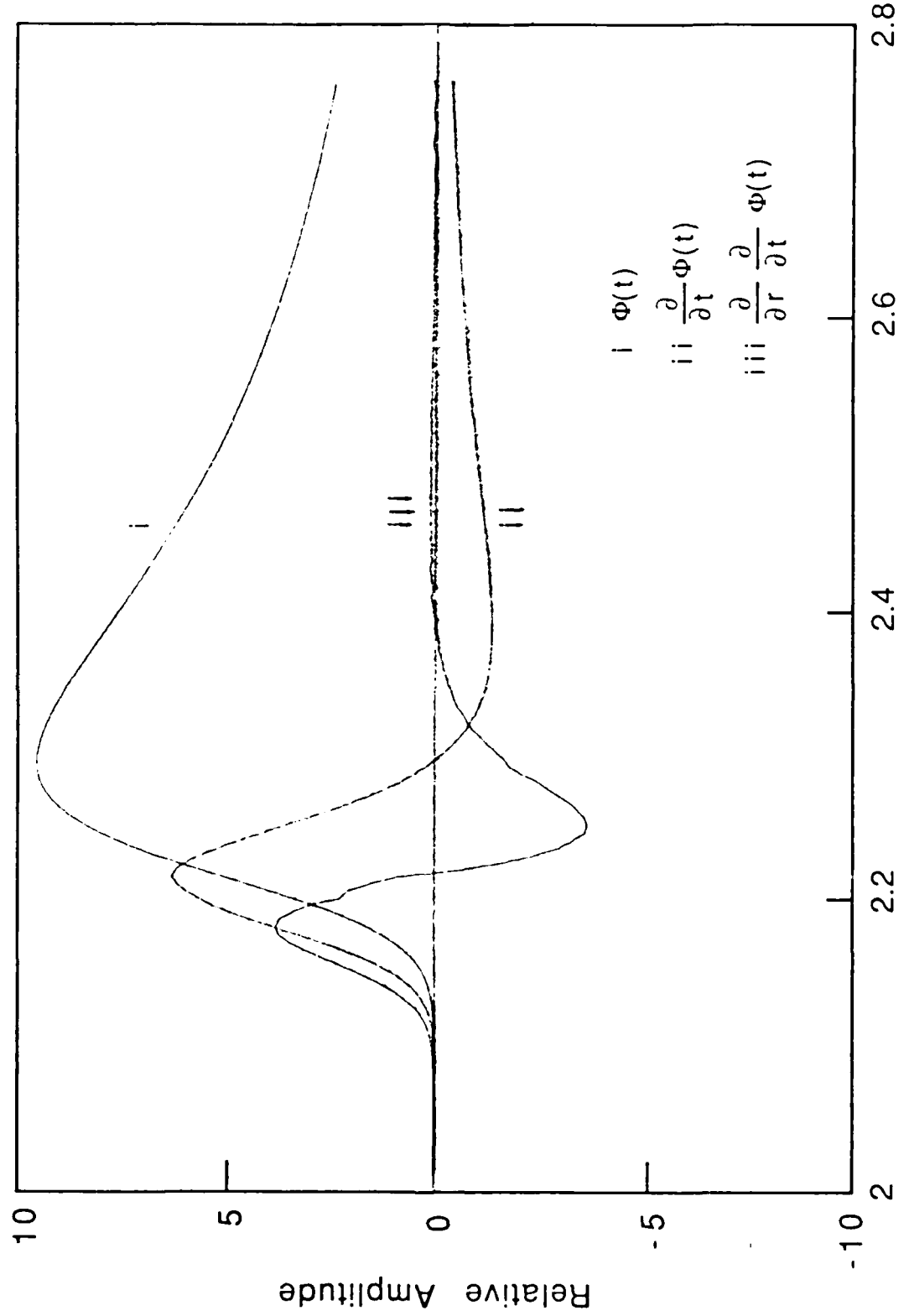
Relative Amplitude
10
5
0
-5
-10
2
2.2
2.4
2.6
2.8
t(μs)
i
ii
iii
i Φ(t)
ii ∂/∂t Φ(t)
iii ∂/∂r ∂/∂t Φ(t)

Figure 8

Figure 9 compares the pressure gradients from Figures 6, 7, and 8 and clearly shows the effect of increasing τ_2. With the first positive peak in each curve normalized to the same magnitude, the negative peak and the second positive peak decrease in amplitude as τ_2 increases while all three peaks broaden in time.

The best fit of the experimental CS_2 waveform was obtained with the rates which produced the curves in Fig. 8. A comparison of the theoretical and experimental curves is shown in Fig. 10. As in Fig. 4, the time scale is for the theoretical curve. The experimental curve is positioned so that the peaks occur at the same point in time. The value of τ_2 for this curve is 91.4 ns. Increasing the value of τ_2 beyond this point continues to decrease the relative magnitude of the negative peak, which the comparison shows to be larger than experimentally observed. However, as τ_2 becomes larger, the initial pressure gradient becomes negative. From equation 29 we can see that, although A_2 is positive and larger in magnitude than A_1, when $\tau_2 >> \tau_1$, the first term becomes dominant and f(t) is negative for small t. Therefore, with the three level system considered here, we are limited in how large the difference in τ_1 and τ_2 can be and still produce the same general shape of the CS_2 signal.

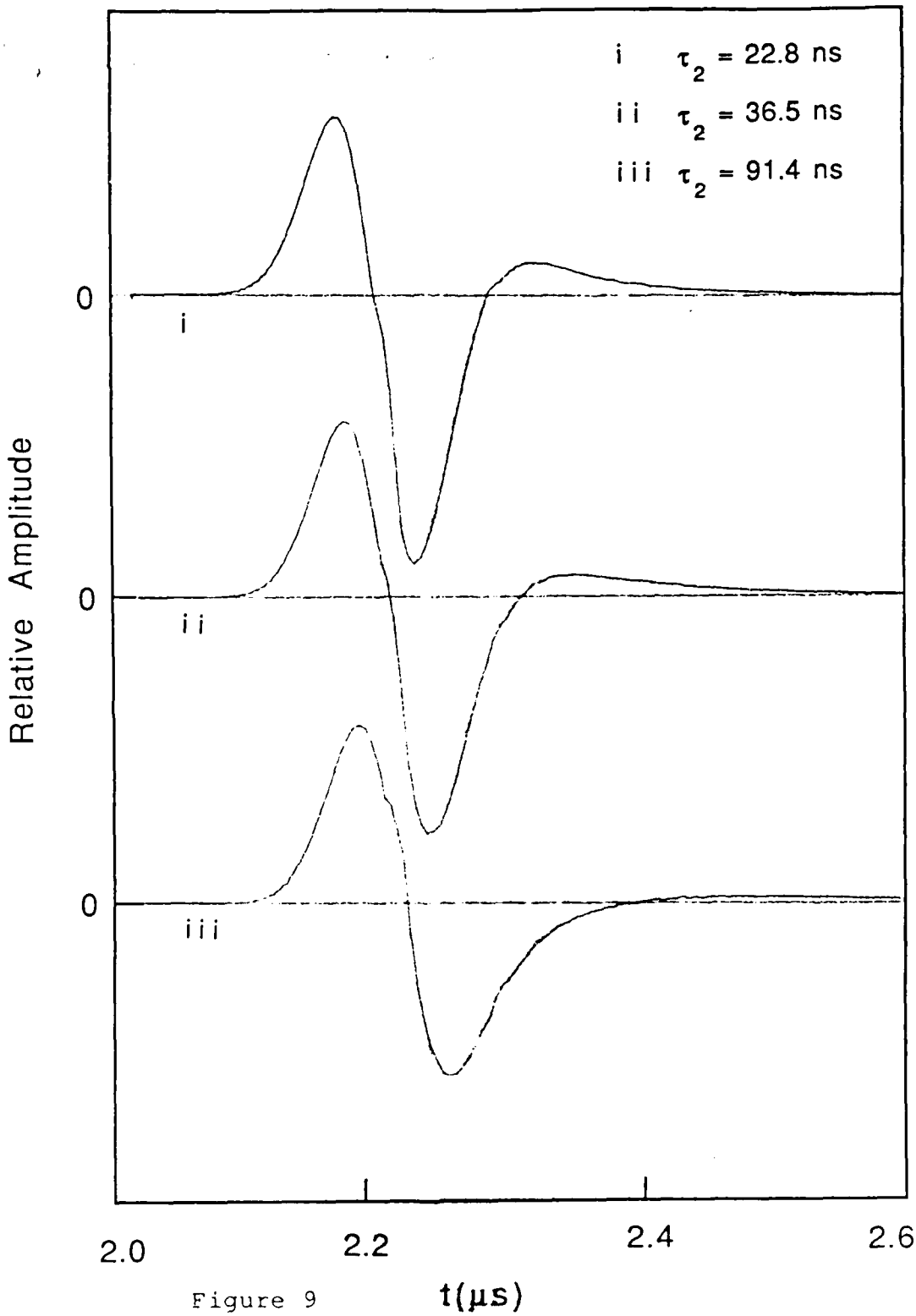
i τ_2 = 22.8 ns
ii τ_2 = 36.5 ns
iii τ_2 = 91.4 ns
Relative Amplitude
0
i
0
ii
0
iii
2.0
2.2
2.4
2.6
t(μs)

Figure 9

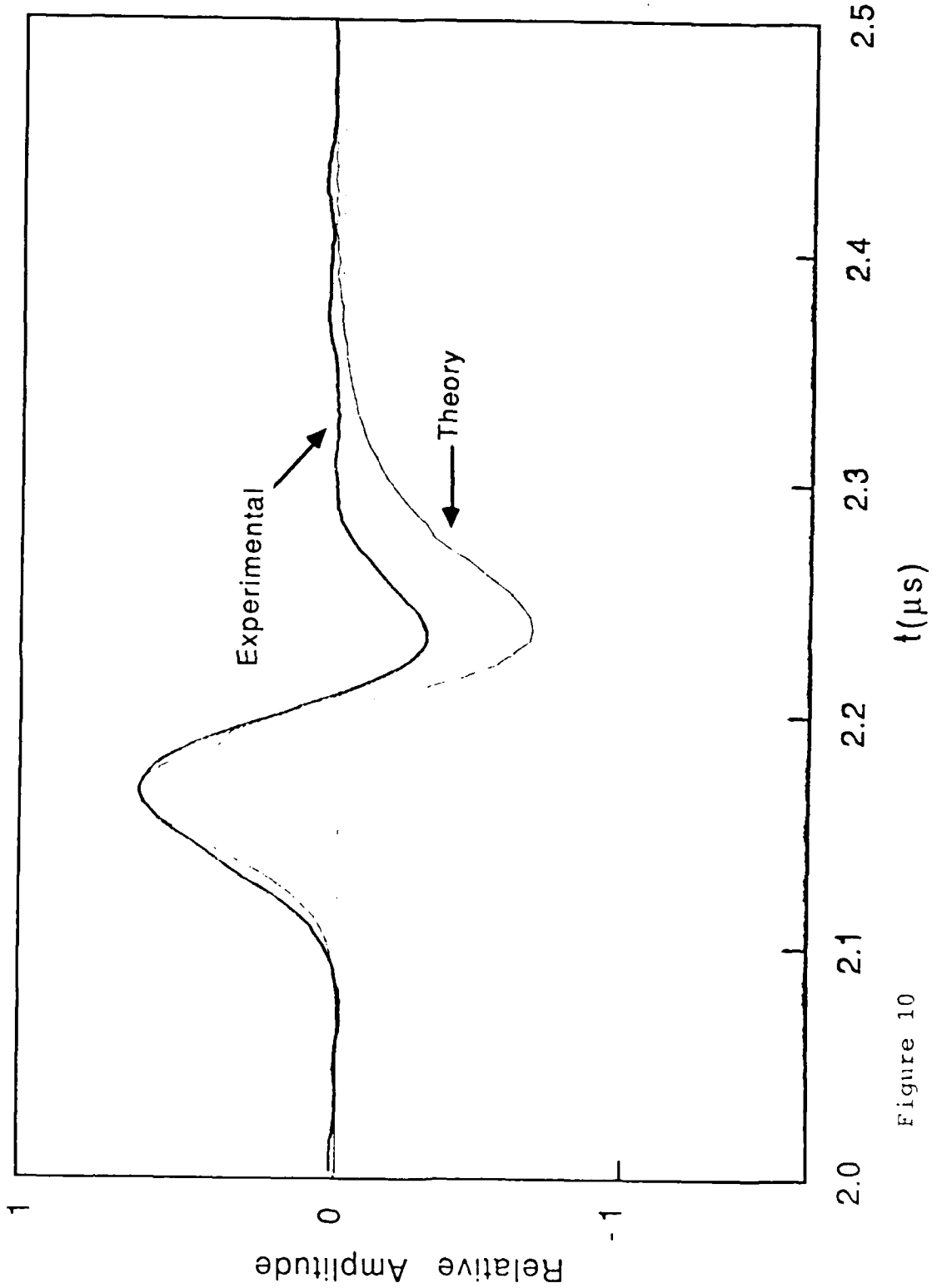
Relative Amplitude
1
0
-1
2.0
2.1
2.2
2.3
2.4
2.5
t(μs)
Experimental
Theory

Figure 10

A better prediction of the optoacoustic signal should be obtainable by considering a more comprehensive reaction scheme than the three level system presented here.

The agreement is better for the early part of the pulse. The same discrepancy in the initial rise that appeared in the propanol signal occurs here, and again could be corrected by modifying the spatial profile function.

From these results we conclude that the optoacoustic effect can be used to investigate relaxation effects in liquids. Obviously, to observe relaxation in most liquids, which have much shorter relaxation times than CS_2, it will be necessary to produce much shorter acoustic pulses than the apparatus used here produces. However, the theoretical calculations show that the effects of relaxation become apparent even for relaxation times less than τ_a for the experiment. Figure 6 shows a distinct difference from Fig. 5 in the latter part of the signal. The longest relaxation time (lowest transition rate) involved in the Fig. 6 calculation was $1/k_{20}$ = 59.3 ns; and τ_2 for this curve was 22.8 ns, which is less than τ_a (~31 ns). An experimental arrangement that allows better focusing of the excitation laser should therefore increase the number of liquids in which it is possible to observe internal relaxation.

Bibliography

1. A.G. Bell. "Production of Sound by Radiant Energy," Amer. J. Sci. 21, 463 (1881).

2. C.K.N. Patel and A.C. Tam. "Pulsed Optoacoustic Spectroscopy of Condensed Matter," Rev. Mod. Phys. 53, 517 (1981).

3. A.C. Tam and W.P. Leung. "Optical Generation and Detection of Acoustic Pulse Profiles in Gases for Novel Ultrasonic Absorption Spectroscopy," Phys. Rev. Lett. 53, 560 (1984).

4. M.H. Ali, H.E. Bass, and H. Yan. "Spectrophone Measurements in Sulfur Hexafluoride," IEEE UFFC-33, 615 (1986).

5. D.A. Hutchins and A.C. Tam. "Pulsed Photoacoustic Materials Characterization," IEEE UFFC-33, 429 (1986).

6. K.F. Herzfeld, T.A. Litovitz. *Absorption and dispersion of Ultrasonic Waves*, Academic Press, New York, 1959, p 90.

7. K.F. Herzfeld, T.A. Litovitz. *Absorption and dispersion of Ultrasonic Waves*, Academic Press, New York, 1959, p 56.

8. H.M. Lai and K. Young. "Theory of the Pulsed Optoacoustic Technique," J. Acoust. Soc. Am. 72, 2000 (1982).

9. J.M. Heritier. "Electrostrictive Limit and Focusing Effects in Pulsed Photoacoustic Detection," Opt. Commun. 44, 267 (1983).

10. J.H. Andreae, E.L. Heasel and J. Lamb. "Ultrasonic Relaxation and the Vibrational Specific Heat of Carbon Disulphide," Proc. Phys. Soc. B69, 625 (1956).

11. K.F. Herzfeld, T.A. Litovitz. *Absorption and dispersion of Ultrasonic Waves*, Academic Press, New York, 1959, p 364.

12. K.F. Herzfeld, T.A. Litovitz. *Absorption and dispersion of Ultrasonic Waves*, Academic Press, New York, 1959, p 58.

13. H.J. Bauer. "Son et Lumiere or the Optoacoustic Effect in Multilevel Systems," J. Chem. Phys. 57, 3130 (1972).

14. G. Herzburg. *Molecular Spectra and Molecular Structure II Infrared and Raman Spectra of Poly-Atomic Molecules*, Van Nostrand Co., Inc., New York, 1945. p 276.

15. M.H. Ali. Ph.D. dissertation, "Spectrophone Measurements in Sulfur Hexafluoride," University of Mississippi, September, 1985.

16. P.M. Morse and H. Feshbach. *Methods of Theoretical Physics*, McGraw Hill, New York, 1953. p 840.

17. B. Sullivan and A.C. Tam. "Profile of Laser-produced Acoustic Pulse in a Liquid," J. Acoust. Soc. Am. 75(2) 437 (1984).

APPENDIX A

ROUTINE FOR CALCULATION OF DIRAC RESPONSE OF THE PROBE BEAM

```
*     'dirac' calculates the dirac response of the
*     probe beam as an integral over z.
*       source is a delta function in time, cylindrically
*       shaped with a gaussian radial profile, exponential
*       decay with depth
*
*     r - radial distance from z axis of source to field
*           point
*     z - depth of field point into medium
*     a - characteristic radius of source
*     c - soundspeed
*     alpha _ absorption coefficient of medium
*             ( 1/alpha = penetration depth )
*     ml - number of a's for which we'll allow contributions
*     nl - number of penetration depths for allowed contri-
*            butions
*             ( ml*a and nl/alpha determine the cutoff pts.
*               of source
*                 intensity is zero for r>mla and z>nl/alpha )
*     ro,zo - source pt. coordinates
*     rho,fee,xi - spherical coordinates with origin at
*                    field pt.
*             (xi=cos(theta))
*     g(ro,zo) - spatial profile function for source
*     U(i) - amplitude of response at t(i)
*             U is double subscripted, calculated at two
*             distant values of r in order to do gradient
*               calculation.
*     point - indicates the value of r at which the
*             calculation is done
*     to - starting time
*     tf - ending time

      real U(2,0:300),t(0:300)
      real r,z,a,c,alpha,ro,zo,rho,xi,fee,g
      real pi,e
      integer i,j,k,s,point
      integer ml,nl,pds
*
      parameter (a=50.e-6, alpha=3.7e+4, c=1140.0 )
      parameter (pi=3.1416, e=2.7183)

      data U,t/903*0.0/
      open(unit=11,file='U1')
      open(unit=12,file='U2')
      open(unit=13,file='t')
```

```
      m1=4
      n1=20

      r=2.5e-3
*     print*,' input r value in meters'
*     read*,r

*     this section determines the first point in time that
* there is a contribution to U ( the shortest distance to
* a source point ) and how big the time increment must be
* to include all of the response.


      to= (r-m1*a)/c
*    for now let total=1500ns to corespond to D-scope
*    pictures (50ns/div)
      total= 1500.0e-9
      dt= total/300
      t(0)=to-dt

*         t(0) is the first point in the file 't'
*       it is placed 1 dt before the first contributing
*       time, consequently U(0) is always 0.0

      write (11,*)U(1,0)
      write (12,*)U(2,0)
      write (13,*)t(0)

*         here we calculate how far along the probe beam we
*     must integrate untill the propagation time is greater
*     than tf=to+500ns.
*
      z=(n1/alpha) + c*sqrt((500.0e-9)**2+2.0*to*500.0e-9)
      print*,' zmax=',z

*     there are z*alpha penetration depths in this distance
*     and we'll have 5 points per penetration depth

      pds = nint(z*alpha)
       dz = 0.2/alpha
      print*,' ',pds,' penetration depths ',5*pds,' z-points'



* as we step through time, each point is associated with the
```

```
* surface of a sphere of radius rho=ct(i).
* we have contributions to phi from source points which lie
* on this surface. (wherever the sphere intersects the
* source distribution.)

* at each point in time we will determine the range of
* fee and xi which are in the source and sum the contributions
* from source pts. in this range.


      do 1100 point=1,2
         r=r+(point-1)*c*dt
      do 1010 s=0,5*pds
         z=s*dz
*     print*,'input z'
*     read*,z
      do 1000 i=1,300
         t(i)=t(0)+i*dt
         rho=c*t(i)

*     given rho, we can determine the limits of xi

                     if (rho.lt.(r-a*ml)) go to 1000
*            case 1
                     if (rho.lt.(r+a*ml)) then
                       ximax=1.0
                       ximin=(r-a*ml)/rho
                     else
*            case 2
                       ximax=(r+a*ml)/rho
                       ximin=(r-a*ml)/rho
                     endif

            dxi =(ximax-ximin)/20
*            in order to do the calculation at the center
*            of each dxi, move the first xi to xi+ dxi/2.0
            ximin= ximin + dxi/2.0

            do 900 j=0,19
               xi= ximin + j*dxi

*           given rho and xi we can determine the limits on fee

*           maximum value of fee is pi/2
*           this section determines the minimum value

                     test1=(a*ml)**2 - (rho*xi)**2 - r**2 +
                         2*r*rho*xi
```

```
                        test2=rho**2*(1-xi**2)

                        if (test1.ge.test2) then
                          minfee=0.0
                        else
                          minfee=acos(sqrt(test1/test2))
                        endif
*               limits on fee are minfee to pi/2 and -minfee to
*               -pi/2  contributions from negative angles will be
*               paired with positives when calculating U.

                        dfee = (pi/2 - minfee)/20.0
                         minfee = minfee + dfee/2

                        do 800 k=0,19
                          fee = minfee + k*dfee


*       now we have rho,xi,fee values
*       calculate ro,zo, and g(ro,zo)
*       ro is independant of the sign of fee.
*       zo has different values for fee and -fee

        ro = sqrt( (rho*xi - r)**2 + (rho*sqrt(1-xi**2)
     i    *cos(fee))**2)

        zo = z + rho*sqrt(1-xi**2)*sin(fee)

*          if zo is out of range don't allow contribution to U
*          go instead to check zo(-fee)
           if (abs(zo).gt.(nl/alpha)) go to 100

        g = e**(-(ro/a)**2 - alpha*(abs(zo)))

        U(point,i) = U(point,i) + t(i)*(c/(4*pi))**2 *
     i     g*dxi*dfee*dz

100     zo = z - rho*sqrt(1-xi**2)*sin(fee)

*          if zo is out of range don't allow contribution to U
*          go instead to get new fee
           if (abs(zo).gt.(nl/alpha)) go to 800

        g= e**(-(ro/a)**2 - alpha*(abs(zo)))

        U(point,i) = U(point,i) + t(i)*(c/(4*pi))**2
     i     * g*dxi*dfee*dz
```

```
800   continue
*     (800 is the end of a fee loop)
900   continue
*     (900 is the end of a xi loop)
1000  continue
*     (1000 completes a pair of U(i),t(i) for one value of z)
1010  continue
*     (1010 completes U(i),t(i))
1100  continue
*     (1100 ends calculation of U for one r value)
*     (write arrays to files)
      do 1002 i=1,300
        write (11,*)U(1,i)
        write (12,*)U(2,i)
        write (13,*)t(i)
1002  continue
      end
```

APPENDIX B

ROUTINE FOR CALCULATION OF POTENTIAL FUNCTION

```
*
*     'duhamel' calculates the potential using duhamel's
*     principle and the dirac response from 'dirac'
*
*        'dirac' computes a 301 point array for U(i),t(i)
*     phi(i) is the integral over tp from 0 to t(i) of
*     U(t(i)-tp)f(tp)dtp
*
*       however U is zero for t less than t(0)
*                          or t(i)-tp less than t(0)
*                          or tp greater than t(i)-t(0)
*       so we set an upper limit for the integral of
*       tp/dtp = (t(i)-t(0))/dtp = i
*
*     phi(i) - potential
*     U(i) - dirac response
*     f - time dependant profile function
*     tau1,tau2 - relaxation times
*     A1,A2 - relaxation strengths
*     tp - integration variable
*

      real phi(2,0:300),U(2,0:300),t(0:300)
      real dt,dtp,tp,f
      real tau1,tau2,A1,A2
      integer i,l,ul,q,point

      open (unit=14,file='phi1')
      open (unit=15,file='phi2')

      data phi/602*0.0/
      open (unit=11,file='U1',status='old')
      open (unit=12,file='U2',status='old')
      open (unit=13,file='t',status='old')
      read(13,*)t(0)

      print*,' input values for tau1,tau2'
      read*,tau1,tau2
*     print*,' input values for A1,A2'
*     read*,A1,A2
      A1=-1.26e-5
      A2= 2.031e-4


      do 1 i=0,300
```

```
        read(11,*)U(1,i)
        read(12,*)U(2,i)
1     continue

      dt=5.e-9
*     note that setting dt=5ns is specialized to form of
*     'dirac' where dt=5ns

      do 100 point=1,2
      do 50 i=0,300
            t(i)=t(0)+i*dt
            ul=i
         do 30 q=1,2
            if (q.eq.1) then
              tau=tau1
              A=A1
            else
              tau=tau2
              A=A2
            endif

*     two loops are included, one for fast relaxations
*     one for slow relaxations
            if (tau.le.2*dt) go to 20

10    continue

            dtp=dt
              tp=0.0

*     the integration is done by the trapezoid rule
              f=(A/tau)
              phi(point,i)=phi(point,i)+U(point,i)*f
     i           *dtp/2.0
*     this is the first term when using the trapezoid rule
*       last term (tp=ul*dtp) will be zero because U(step,0)
*       is zero
            do 15 l=1,ul
              tp=l*d
                f=(A/tau)*exp(-tp/tau)
              if (tp/tau.gt.20.0) go to 19
*             because f will be small for remaining l's
                phi(step,i)=phi(step,i) + U(step,ul-l)*f*dtp

15    continue
19    go to 30
20    continue
```

```
*               start here for fast relaxations, linear
*               interpolation is done between U(i) and U(i+1)
      dtp=dt/25

      do 30 l=1,ul

               slope=(U(step,ul-l+1)-U(step,ul-l))/25
               tq=(l-1)*dt

               tp=tq
               f=(A/tau)*exp(-tp/tau)
               phi(step,i)=phi(step,i)+U(step,ul-l+1)*f*dtp/2.0
               tp=tq+25*dtp
               f=(A/tau)*exp(-tp/tau)
               phi(step,i)=phi(step,i)+U(step,ul-l)*f*dtp/2.0


               do 25 n=1,24
                 tp=tq+n*dtp
                 f=(A/tau)*exp(-tp/tau)
                   if (tp/tau.gt.20) go to 30


               phi(step,i)=phi(step,i)+(U(step,ul-l+1)-slope*n)
     i            *f*dtp

25    continue

30    continue
50    continue
100   continue
      do 101 i=0,300
        write(14,*)phi(1,i)
        write(15,*)phi(2,i)
101   continue
      end
```

APPENDIX C

ROUTINE FOR CALCULATION OF ACOUSTIC PRESSURE

```
*       numerically differentiates the potential
*       to get the pressure


        real phi1(0:100),phi2(0:100),t(0:100)
        real pres1(0:99),pres2(0:99),tp(0:99)
        real delta
        integer n


        open (unit=13,file='t',status='old')
        open (unit=14,file='phi1',status='old')
        open (unit=15,file='phi2',status='old')
        do 900 n=0,100
        read(14,*)phi1(n)
        read(15,*)phi2(n)
        read(13,*)t(n)
900     continue


        open (unit=16,file='tp',status='new')
        open (unit=17,file='pres1',status='new')
        open (unit=18,file='pres2',status='new')

        do 1000 n=1,100
                delta= (t(n)-t(n-1))
                pres1(n-1)= (phi1(n)-phi1(n-1))/delta
                pres2(n-1)= (phi2(n)-phi2(n-1))/delta
        write(17,*)pres1(n-1)
        write(18,*)pres2(n-1)
                tp(n-1)= t(n-1) + delta/2.0
        write(16,*)tp(n-1)
1000    continue
        end
```

APPENDIX D

ROUTINE FOR CALCULATION OF GRADIENT OF THE ACOUSTIC PRESSURE

```
*       numerically differentiates the pressure
*       to get it's gradient


        real pres1(0:99),pres2(0:99),tp(0:99)
        real dpres(0:99),delta
        integer n


        delta=(1140.0*5.e-9)
        open (unit=16,file='tp',status='old')
        open (unit=17,file='pres1',status='old')
        open (unit=18,file='pres2',status='old')

        do 900 n=0,99
        read(16,*)tp(n)
        read(17,*)pres1(n)
        read(18,*)pres2(n)
900     continue


        open (unit=19,file='dpres',status='new')

        do 1000 n=0,99
                dpres(n)=(pres1(n)-pres2(n))/delta
                write(19,*)dpres(n)
1000    continue
        end
```

END

DATE

FILMED

5-88

DTIC